Rapamycin rejuvenates oral health in aging mice

Jonathan Y. An[1,2], Kristopher A. Kerns[1,6], Andrew Ouellette[3], Laura Robinson[3], Doug Morris[3], Catherine Kaczorowski[3], So-Il Park[2], Title Mekvanich[2], Alex Kang[2], Jeffrey S. McLean[1,5], Timothy C. Cox[4,#], Matt Kaeberlein[1,2,*]

1 Department of Oral Health Sciences, University of Washington, Seattle, WA, USA
2 Department of Pathology, University of Washington, Seattle, WA, USA
3 The Jackson Laboratory, Bar Harbor, ME, USA
4 Department of Pediatrics, University of Washington, & Seattle Children's Research Institute, Seattle, WA, USA
5 Department of Periodontics, University of Washington, Seattle, WA, USA
6 Center of Excellence in Maternal and Child Health, University of Washington, Seattle, WA, USA

[#]current address: Department of Oral & Craniofacial Science, School of Dentistry, University of Missouri-Kansas City, Kansas City, MO, USA

*Corresponding author: kaeber@uw.edu

Single Sentence Summary: Short-term treatment with rapamycin reverses periodontal bone loss, attenuates inflammation, and remodels the oral microbiome toward a more youthful state.

Abstract: Periodontal disease is an age-associated disorder clinically defined by periodontal bone loss, inflammation of the specialized tissues that surround and support the tooth, and microbiome dysbiosis. Currently, there is no therapy for reversing periodontal disease, and treatment is generally restricted to preventive measures or tooth extraction. The FDA-approved drug rapamycin slows aging and extends lifespan in multiple organisms, including mice. Here we demonstrate that short-term treatment with rapamycin rejuvenates the aged oral cavity of elderly mice, including regeneration of periodontal bone, attenuation of gingival and periodontal bone inflammation, and revertive shift of the oral microbiome toward a more youthful composition. This provides a geroscience strategy to potentially rejuvenate oral health and reverse periodontal disease in the elderly.

Main Text: Old age is associated with failure to maintain homeostasis resulting in degradation of cellular maintenance and repair processes (*1*) and is the single greatest risk factor for many human diseases including cardiovascular disorders, dementias, diabetes, and most cancers (*2, 3*). Interventions that target specific aging hallmarks have been shown to delay or prevent age-related disorders and extend lifespan in model organisms (*4*). Rapamycin, an FDA approved drug which directly inhibits the mechanistic target of rapamycin complex I (mTORC1), is one such intervention that extends lifespan and ameliorates a variety of age-related phenotypes (*5*). In mice, rapamycin extends lifespan when administered beginning at 9 or 20 months of age (*6*), and short-term treatments ranging from 6-12 weeks during adulthood have been shown to increase lifespan (*7*), improve cardiac function (*8, 9*) and restore immune function as measured by vaccine response (*10*). Initial indications suggest that mTORC1 inhibition can also reverse declines in age-related heart function in companion dogs and age-related immune function (*11, 12*) and skin aging (*13*) in humans.

The American Academy of Periodontology (AAP) defines periodontitis as inflammation of the periodontium, the specialized tissue surrounding and supporting the tooth structure, resulting in clinical attachment loss, alveolar (periodontal) bone loss and periodontal pocketing, and associated variability in the oral microbial (*14*). Most recent epidemiologic data in the U.S. population suggests that more than 60% of adults aged 65 years and older have periodontitis (*15, 16*), and diagnosis with periodontal disease is associated with increased risk for other age-related conditions including heart disease, diabetes, and Alzheimer's disease (*17-19*). We have previously observed that aged mice treated with rapamycin have greater levels of periodontal bone than control animals (*20*), suggesting that inhibition of mTOR may delay age-related periodontal disease.

In order to understand potential mechanisms by which aging and mTOR activity influence oral health, we assessed whether transient rapamycin treatment is sufficient to regrow periodontal bone in aged animals. Two cohorts of animals were used for these studies: NIA-UW mice housed at the University of Washington and JAX mice housed at The Jackson Laboratory (see Methods). We used microCT (μCT) imaging to measure the amount of periodontal bone present in the maxilla and mandible of young (6 month), adult (13 month), and old

(20 month) mice from the NIA-UW cohort (fig. S1). The amount of periodontal bone for the maxilla and mandible of each animal was calculated as the distance from the cementoenamel junction (CEJ) to alveolar bone crest (ABC) for 16 landmarked sites each on the buccal aspect of the maxillary and mandibular periodontium (fig. S2). Thus, larger values represent greater bone loss. As expected, there was a significant loss of periodontal bone with age in the NIA-UW cohort (Fig. 1, A and B). Mice treated with rapamycin for 8 weeks had significantly more bone at the end of the treatment period compared to mice that received the control diet (eudragit). To determine whether the increase in periodontal bone upon rapamycin treatment reflects attenuation of bone loss or growth of new bone, we performed μCT imaging on mice before and after treatment in the JAX cohort. Old mice randomized into either the eudragit control or rapamycin treatment groups had significantly less periodontal bone than young mice prior to the treatment period (Fig. 1F). After 8 weeks, the rapamycin treated mice had significantly more periodontal bone compared to eudragit controls and also compared to the pre-treatment levels for the same animals (Fig. 1, D to F). The presence of new bone following rapamycin treatment can be observed by comparison of μCT images from the same animals before and after treatment (Fig. 1, D and E).

Normal bone homeostasis results from a balance between new bone growth and bone resorption, which is reflected by the ratio of RANKL (receptor-activator of nuclear factor-κB ligand) to OPG (osteoprotegerin), and dysregulation of this balance contributes to bone loss in periodontitis (*21*). Consistent with bone loss during aging, we detected significantly greater levels of RANKL in old animals of both cohorts compared to young animals (Fig. 2, A and B) OPG levels remained relatively stable, resulting in an increase in the RANKL:OPG ratio indicative of bone resorption exceeding bone formation (Fig. 2C). These age-associated defects in bone homeostasis were suppressed by eight weeks of rapamycin treatment (Fig. 3). In addition to increased RANKL:OPG ratio, a significant increase in $TRAP^+$ cells was also observed in periodontal bone with age (Fig. 3, D and E). TRAP (tartrate-resistant acid phosphatase) is a histochemical marker of bone resorbing osteoclasts (*22, 23*). Rapamycin treatment for eight weeks also decreased $TRAP^+$ cells. Together, our data indicate that rapamycin reverses periodontal bone loss in the aging murine oral cavity at least in part through inhibition of bone resorption.

Along with bone loss, gingival inflammation is a defining feature of periodontal disease. Aging is also associated with chronic accumulation of pro-inflammatory factors, a collective term referred to as inflammaging (*24-27*). The nuclear factor-κB (NF-κB) is a hub of immune and inflammatory response activated both during normal aging and as a consequence of periodontal disease (*28-31*) . We first evaluated the NF-κB hub through NF-κB p65 and IκBα expressions levels. The NF-κB heterodimer consists of RelA (or p65) and p50. IκBα functions as a negative regulator of NF-κB by sequestering it in the cytoplasm. Degradation of IκBα or phosphorylated-IκBα leads to nuclear localization of NF-κB subunits which induce expression of target inflammatory genes, such as TNF-α and IL-1β (*31*). In both the gingival tissue and periodontal bone, there was an increase in p65 expression with corresponding decrease of IκBα levels, indicating an age-associated increase in NF-κB inflammatory signaling in the periodontium (Fig. 3, A and B). Eight weeks of rapamycin treatment was sufficient to reverse these changes. We also examined the levels of inflammatory cytokines in the oral cavity associated with normative aging and rapamycin treatment in mice. Consistent with the increase in NF-κB signaling, we found elevated expression of several cytokines in both the gingival tissue and the periodontal bone (Fig. 3, E and F). Eight weeks of rapamycin treatment reversed most age-associated chemokine and cytokine changes in both the gingival tissue and periodontal bone. Thus, transient treatment with rapamycin during middle-age can largely restore a youthful inflammatory state in both the gingiva and periodontal bone of mice.

Dysbiotic shifts in the oral microbiome are thought to play a significant role in the progression of periodontal disease in humans. We and others have previously shown that rapamycin treatment can remodel the gut microbiome in mice (*32-34*); however, the effect of rapamycin on the oral microbiome has not been explored. Therefore, we sought to evaluate effects of rapamycin on the aged oral microbiome using 16S rRNA gene sequencing and Amplicon Sequence Variant (ASV) analysis approach. Examination of the alpha diversity of the oral cavity illustrated a significant increase in species richness during aging that rapamycin treatment impacted (Fig. 4A, fig. S3). Among the most notable alterations in taxonomic abundance between groups was the reduction of *Bacteroidetes* phylum that had increased with age but reduced in the rapamycin-treated old animals (Fig. 4B, fig. S4). The *Bacteroidetes* phylum consists of over 7000 different species (*35*) and includes bacteria associated with human periodontal disease such as *Porphyromonas gingivalis, Treponema denticola,* and *Bacteroides forsythus* (*36-38*). Further, both the *Firmicutes* and *Proteobacteria* phyla also showed a significant difference that was age and treatment dependent (Fig. 4B). In order to assess whether rapamycin is shifting the composition back towards a youthful state, we evaluated the beta diversity using weighted UniFrac

distances. We discovered a significant separation of the oral microbiome between old control and old rapamycin-treated animals, while no significant differences were observed between young mice and old rapamycin-treated mice (Fig. 4C). Overall, we observed no significant differences in alpha diversity, beta diversity, nor relative taxonomic abundance between young mice and old mice treated with rapamycin, suggesting an eight-week treatment with rapamycin reverted the old oral microbiome to a more youthful state. This observation is further supported when analysis of the samples is performed independently by facility (UW-NIA or JAX) (fig. S5).

Taken together, our data demonstrate that a short-term treatment with rapamycin in aged mice is sufficient to target three clinically defining features of periodontal disease: periodontal bone loss, periodontal inflammation, and pathogenic changes to the oral microbiome. To the best of our knowledge, this is the first report of rejuvenation in the aged oral cavity. It will be important in future studies to determine whether these effects are mediated through local inhibition of mTORC1 in the gingiva and periodontal bone or through systemic effects on immune function or other tissues. Likewise, it will be of interest to understand whether additional features of oral health that are known to decline with age, such as salivary function, are improved by rapamycin treatment. Finally, these results suggest the intriguing likelihood that additional geroscience interventions, such clearance of senescent cells, may phenocopy the effects of rapamycin in this context. Such interventions could pave the way for the first effective treatments to reverse periodontal disease and improve oral health in the elderly.

Acknowledgements: The authors to would like to thank the Karl F. Liem Facility at Friday Harbor Laboratories, and Ryan Anderson on his guidance at Seattle Children's Research Institute. **Funding:** This work was supported by NIDCR Dental Scientist Fellowship DE027254 (JYA) and Dentsply Sirona Research Award (JYA), in part funded by NIH NIDCR Awards DE023810 and DE020102 (JSM), National Institute on Aging grants R01AG054180 (CCK), The Jackson Laboratory Nathan Shock Center on Aging grant P30AG038070 (GC, LP, RC) and P30AG038070 pilot award (CCK), the National Center For Advancing Translational Sciences of the NIH under Award Number TL1 TR002318 (KAK). **Author contributions:** J.Y.A led the project, and conceptualized, investigated, curated data, analyzed, and wrote the manuscript. K.A.K contributed to analysis and investigation on the oral microbiome and 16s rRNA sequencing results; A.O, L.R and C.K contributed to project administration, resources, and investigation for the JAX colonies; D.M. contributed to data curation and methodology; S.P., T.M., and A.K contributed to analysis; J.S.M contributed to formal analysis, resources for 16s rRNA sequencing; T.C.C contributed to the microCT analysis; M.K contributed to conceptualization, investigation, funding acquisition, supervision, and validation. J.Y.A, K.A.K, C.K., J.S.M., M.K contributed equally to reviewing and editing the writing of the article. **Competing Interests:** The authors declare no competing interests. **Data and materials availability:** All data is available in the manuscript or the supplemental materials. The V4-16s rDNA sequences in raw format, prior to post-processing and data analysis, have been deposited at the European Nucleotide Archive (ENA) under study accession no. PRJEB35672.

References:

1. C. López-Otín, M. A. Blasco, L. Partridge, M. Serrano, G. Kroemer, in *Cell*. (2013), vol. 153.
2. F. Sierra, R. Kohanski, Geroscience and the trans-NIH Geroscience Interest Group, GSIG. *Geroscience* **39**, 1-5 (2017).
3. B. K. Kennedy *et al.*, Geroscience: linking aging to chronic disease. *Cell* **159**, 709-713 (2014).
4. M. Kaeberlein, P. S. Rabinovitch, G. M. Martin, Healthy Aging: The Ultimate Preventative Medicine. *Science* **350**, 1191-1193 (2015).
5. S. C. Johnson, P. S. Rabinovitch, M. Kaeberlein, mTOR is a key modulator of ageing and age-related disease. *Nature* **493**, 338-345 (2013).
6. D. E. Harrison *et al.*, Rapamycin fed late in life extends lifespan in genetically heterogeneous mice. *Nature* **460**, 392-395 (2009).
7. A. Bitto *et al.*, Transient rapamycin treatment can increase lifespan and healthspan in middle-aged mice. *eLife* **5**, e16351 (2016).
8. J. M. Flynn *et al.*, Late-life rapamycin treatment reverses age-related heart dysfunction. *Aging Cell* **12**, 851-862 (2013).
9. D. F. Dai *et al.*, Altered proteome turnover and remodeling by short-term caloric restriction or rapamycin rejuvenate the aging heart. *Aging Cell* **13**, 529-539 (2014).

10. C. Chen, Y. Liu, P. Zheng, mTOR regulation and therapeutic rejuvenation of aging hematopoietic stem cells. *Sci Signal* **2**, ra75 (2009).
11. J. B. Mannick *et al.*, mTOR inhibition improves immune function in the elderly. *Science Translational Medicine* **6**, 268ra179--268ra179 (2014).
12. J. B. Mannick *et al.*, TORC1 inhibition enhances immune function and reduces infections in the elderly. *Sci Transl Med* **10**, (2018).
13. C. L. Chung *et al.*, Topical rapamycin reduces markers of senescence and aging in human skin: an exploratory, prospective, randomized trial. *Geroscience*, (2019).
14. P. American Academy of. (2019), vol. 2019.
15. P. I. Eke *et al.*, Prevalence of periodontitis in adults in the United States: 2009 and 2010. *J Dent Res* **91**, 914-920 (2012).
16. P. I. Eke *et al.*, Update on Prevalence of Periodontitis in Adults in the United States: NHANES 2009 to 2012. *J Periodontol* **86**, 611-622 (2015).
17. J. A. Gil-Montoya, A. L. de Mello, R. Barrios, M. A. Gonzalez-Moles, M. Bravo, Oral health in the elderly patient and its impact on general well-being: a nonsystematic review. *Clinical interventions in aging* **10**, 461-467 (2015).
18. J. Kim, S. Amar, Periodontal disease and systemic conditions: a bidirectional relationship. *Odontology* **94**, 10-21 (2006).
19. P. A. Razak *et al.*, Geriatric oral health: a review article. *J Int Oral Health* **6**, 110-116 (2014).
20. J. Y. An *et al.*, Rapamycin treatment attenuates age-associated periodontitis in mice. *Geroscience* **39**, 457-463 (2017).
21. R. P. Darveau, Periodontitis: a polymicrobial disruption of host homeostasis. *Nat Rev Microbiol* **8**, 481-490 (2010).
22. A. R. Hayman, Tartrate-resistant acid phosphatase (TRAP) and the osteoclast/immune cell dichotomy. *Autoimmunity* **41**, 218-223 (2008).
23. P. Ballanti *et al.*, Tartrate-resistant acid phosphate activity as osteoclastic marker: sensitivity of cytochemical assessment and serum assay in comparison with standardized osteoclast histomorphometry. *Osteoporos Int* **7**, 39-43 (1997).
24. H. Y. Chung *et al.*, Molecular inflammation: underpinnings of aging and age-related diseases. *Ageing Res Rev* **8**, 18-30 (2009).
25. C. Franceschi, E. Ottaviani, Stress, inflammation and natural immunity in the aging process: a new theory. *Aging (Milano)* **9**, 30-31 (1997).
26. C. Franceschi *et al.*, Inflamm-aging. An evolutionary perspective on immunosenescence. *Ann N Y Acad Sci* **908**, 244-254 (2000).
27. M. De Martinis, C. Franceschi, D. Monti, L. Ginaldi, in *FEBS Letters*. (2005), vol. 579, pp. 2035-2039.
28. T. Arabaci *et al.*, Immunohistochemical and Stereologic Analysis of NF-kappaB Activation in Chronic Periodontitis. *Eur J Dent* **4**, 454-461 (2010).
29. R. Ambili, P. Janam, A critique on nuclear factor-kappa B and signal transducer and activator of transcription 3: The key transcription factors in periodontal pathogenesis. *J Indian Soc Periodontol* **21**, 350-356 (2017).
30. Y. Abu-Amer, NF-kappaB signaling and bone resorption. *Osteoporos Int* **24**, 2377-2386 (2013).
31. T. Liu, L. Zhang, D. Joo, S. C. Sun, NF-kappaB signaling in inflammation. *Signal Transduct Target Ther* **2**, (2017).
32. A. Bitto *et al.*, Transient rapamycin treatment can increase lifespan and healthspan in middle-aged mice. *Elife* **5**, (2016).
33. M. J. Jung *et al.*, Chronic Repression of mTOR Complex 2 Induces Changes in the Gut Microbiota of Diet-induced Obese Mice. *Sci Rep* **6**, 30887 (2016).
34. V. Hurez *et al.*, Chronic mTOR inhibition in mice with rapamycin alters T, B, myeloid, and innate lymphoid cells and gut flora and prolongs life of immune-deficient mice. *Aging Cell* **14**, 945-956 (2015).
35. F. Thomas, J. H. Hehemann, E. Rebuffet, M. Czjzek, G. Michel, Environmental and gut bacteroidetes: the food connection. *Front Microbiol* **2**, 93 (2011).
36. A. J. van Winkelhoff, B. G. Loos, W. A. van der Reijden, U. van der Velden, Porphyromonas gingivalis, Bacteroides forsythus and other putative periodontal pathogens in subjects with and without periodontal destruction. *J Clin Periodontol* **29**, 1023-1028 (2002).
37. P. J. Torres, J. Thompson, J. S. McLean, S. T. Kelley, A. Edlund, Discovery of a Novel Periodontal Disease-Associated Bacterium. *Microb Ecol* **77**, 267-276 (2019).

38. S. S. Socransky, A. D. Haffajee, M. A. Cugini, C. Smith, R. L. Kent, Jr., Microbial complexes in subgingival plaque. *J Clin Periodontol* **25**, 134-144 (1998).
39. J. Han, P. Wang, S. Ge, The microbial community shifts of subgingival plaque in patients with generalized aggressive periodontitis following non-surgical periodontal therapy: a pilot study. *Oncotarget* **8**, 10609-10619 (2017).
40. A. L. Griffen *et al.*, Distinct and complex bacterial profiles in human periodontitis and health revealed by 16S pyrosequencing. *ISME J* **6**, 1176-1185 (2012).
41. R. A. Miller *et al.*, Rapamycin-mediated lifespan increase in mice is dose and sex dependent and metabolically distinct from dietary restriction. *Aging Cell* **13**, 468-477 (2014).
42. Y. Zhang *et al.*, Rapamycin extends life and health in C57BL/6 mice. *J Gerontol A Biol Sci Med Sci* **69**, 119-130 (2014).
43. A. Limaye, *Drishti: a volume exploration and presentation tool*. SPIE Optical Engineering + Applications (SPIE, 2012), vol. 8506.
44. B. J. Callahan *et al.*, DADA2: High-resolution sample inference from Illumina amplicon data. *Nat Methods* **13**, 581-583 (2016).
45. I. F. Escapa *et al.*, New Insights into Human Nostril Microbiome from the Expanded Human Oral Microbiome Database (eHOMD): a Resource for the Microbiome of the Human Aerodigestive Tract. *mSystems* **3**, (2018).
46. P. J. McMurdie, S. Holmes, phyloseq: an R package for reproducible interactive analysis and graphics of microbiome census data. *PLoS One* **8**, e61217 (2013).
47. T. Metsalu, J. Vilo, ClustVis: a web tool for visualizing clustering of multivariate data using Principal Component Analysis and heatmap. *Nucleic Acids Res* **43**, W566-570 (2015).
48. H. Wickham, in *Use R!* (Springer,, Switzerland, 2016), pp. 1 online resource.
49. K. R. Andersen KS, Karst SM, Albertsen M, ampvis2: an R package to analyse and visualize 16S rRNA amplicon data. *bioRxiv*, (2018).
50. B. F. Oksanen J, Friendly M, Kindt R, Legendre P, McGlinn D, Minchin PR, O'Hara RB, , S. P. Simpson GL, Stevens MHH, Szoecs E, Wagner H., vegan: Community Ecology Package. R package. (2019).
51. D. S. Bougeard S, Supervised Multiblock Analysis in R with the ade4 Package. *Journal of Statistical Software* **86**, 1-17 (2018).

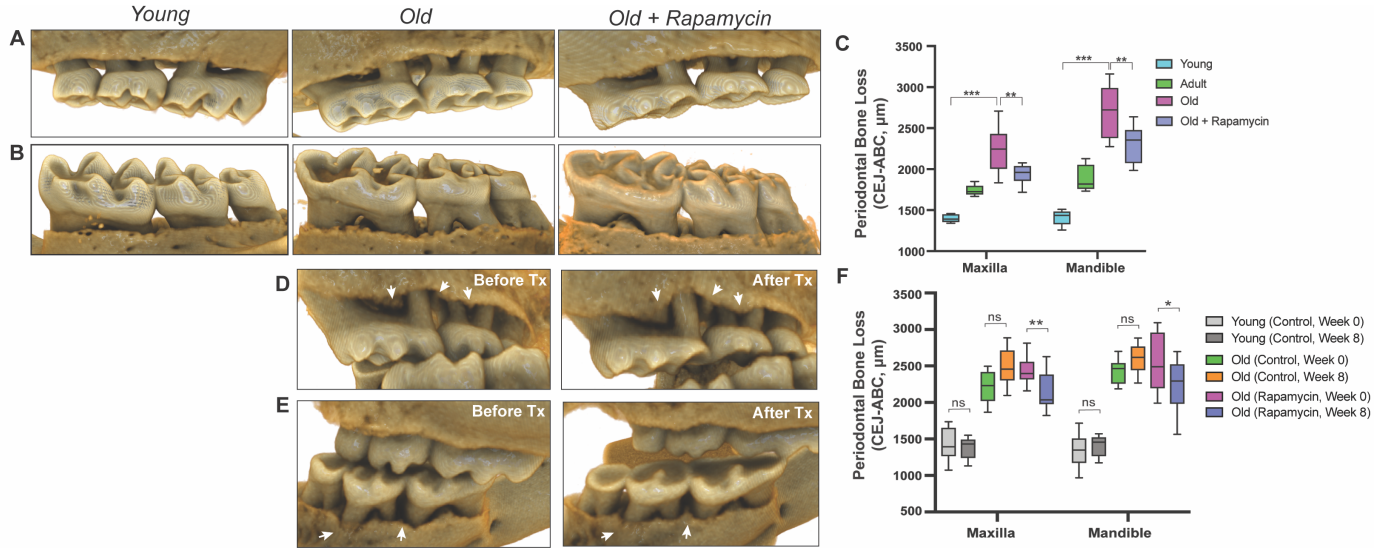

Fig. 1. Rapamycin reverses age-associated periodontal bone loss (NIA-UW and JAX). (A and B) Representative images of NIA-UW (A) maxillary and (B) mandibular teeth of Young, Old, and Old treated with 42ppm eRAPA (rapamycin) revealing age-associated periodontal bone loss. 8 weeks of rapamycin attenuated periodontal bone loss. **(C)** Box-and-whiskers plots shows median, 25th and 75th percentile with whiskers at the 5th and 95th percentile. Statistical analysis was completed using unpaired t-test, with p-values < 0.05 were considered statistically significant. * $p < 0.05$, ** $p < 0.01$, *** $p < 0.005$ **(D and E)** Representative images of the (D) maxillary and (E) mandibular teeth from the same animal in the JAX cohort before treatment (labeled Old) and after 8 weeks of 42ppm eRAPA (labeled Old+Rapamycin). On both the maxilla and mandible, there is periodontal bone loss around and in-between the molars, but after 8 weeks of 42ppm eRAPA the bone loss is reversed. White arrowheads indicate areas of bone loss and bone loss reversal **(F)** Box-and-whiskers plots shows median, 25th and 75th percentile with whiskers at the 5th and 95th percentile. Longitudinal comparison was completed with the same animal at baseline or after 8 weeks with either eudragit (control) or 42ppm eRAPA (rapamycin). Statistical analysis was completed using paired t-test, with p-values < 0.05 were considered statistically significant. * $p<0.05$, ** $p<0.01$

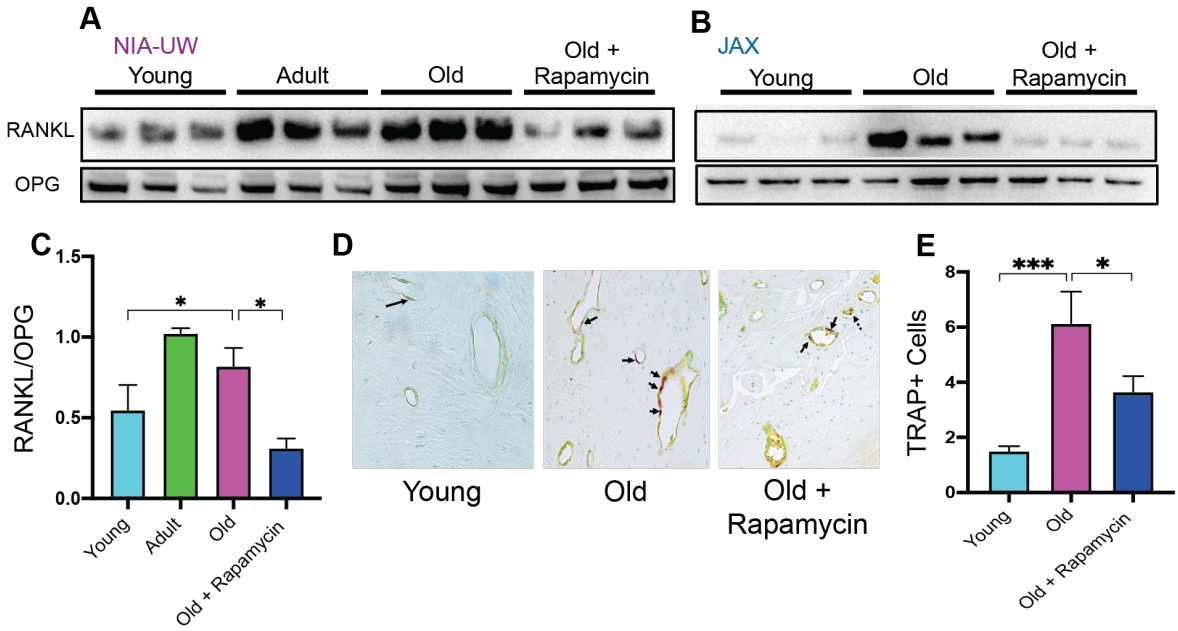

Fig. 2. Rapamycin attenuates age-associated increase in RANKL expression and TRAP+ cells in periodontal bone. (A and B) RANKL and OPG expression was determined by Western blot analysis of total lysates from the periodontal bone of aged animals (Young, Adult, and Old) and Old animals treated for 8 weeks with 42ppm rapamycin (eRAPA). The periodontal bone within both the NIA-UW and JAX Colonies showed an increased expression of RANKL while 8 weeks of rapamycin treatment ameliorated the increased RANKL expression. Each lane represents individual periodontal bone samples. **(C)** Quantification of RANKL/OPG of the NIA-UW Western blot analysis. **(D)** Representative histological sections of the alveolar bone furcation that have undergone TRAP azo-dye staining with FastGreen counterstain. **(E)** Enumeration of $TRAP^+$ cells within the periodontal bone from two-independent observers reveals an increase number of $TRAP^+$ cells with age and diminishes with rapamycin treatment. Statistical analysis completed with unpaired t-test, with significance set to $p<0.05$. * $p<0.05$, ** $p<0.01$, *** $p<0.005$

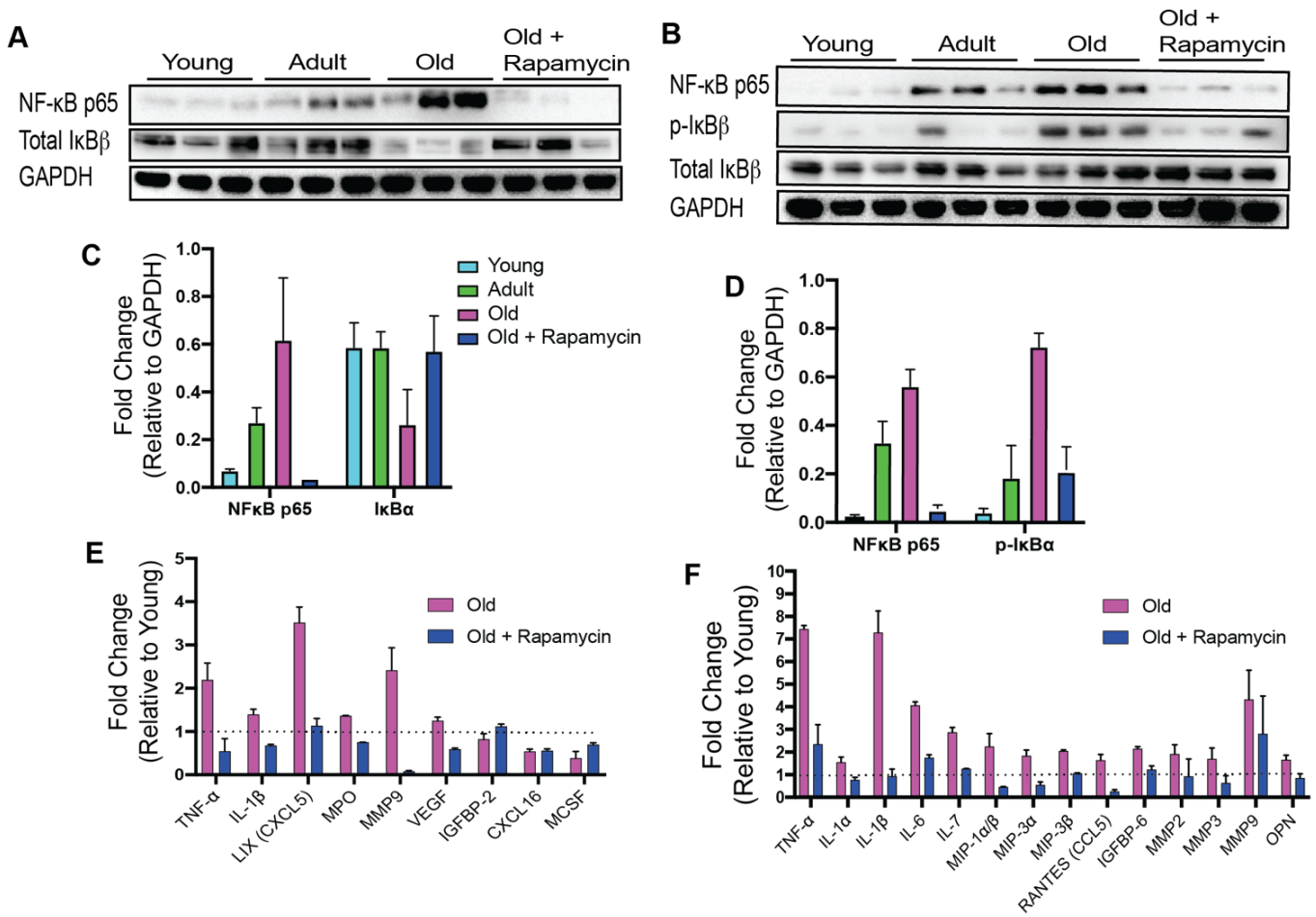

Fig. 3. Rapamycin alters increased NF- κB expression and inflammatory cytokine profiles in periodontium (**A and C)** NF- κB p65 and IκBα expression was determined by Western blot analysis of total lysates from the gingiva and periodontal bone **(B and D)** of aged animals (Young, Adult, and Old) and Old animals treated for 8 weeks with rapamycin (42ppm eRAPA). GAPDH was used a loading control. Both in the aging gingiva and periodontal bone, there is an overall increased expression of NF- κ B p65 with corresponding alteration of IκBα or p- IκBα. 8 weeks of 42ppm eRAPA treatment attenuates the altered changes seen with the increased NF- κB p65 expression. For the gingiva, each lane represents gingiva from animals co-housed (n=1-2), and each lane for the periodontal bone western blot represents individual samples. **(E and F)** Protein expression levels of mouse cytokines and chemokines was determined by a spotted nitrocellulose membrane assay (Proteome Profiler Mouse, R&D Systems) by loading pooled samples from **(E)** gingiva and **(F)** periodontal bone of Young and Old (Control, Eudragit), and Old animals treated for 8 weeks with rapamycin (42ppm eRAPA). Data is shown per manufacture's protocol, with fold-change relative to Young (Set to 1), expressed as mean ± SEM. Only data showing statistical significance set to $p < 0.05$, except CXCL16 and MCSF **(E).**

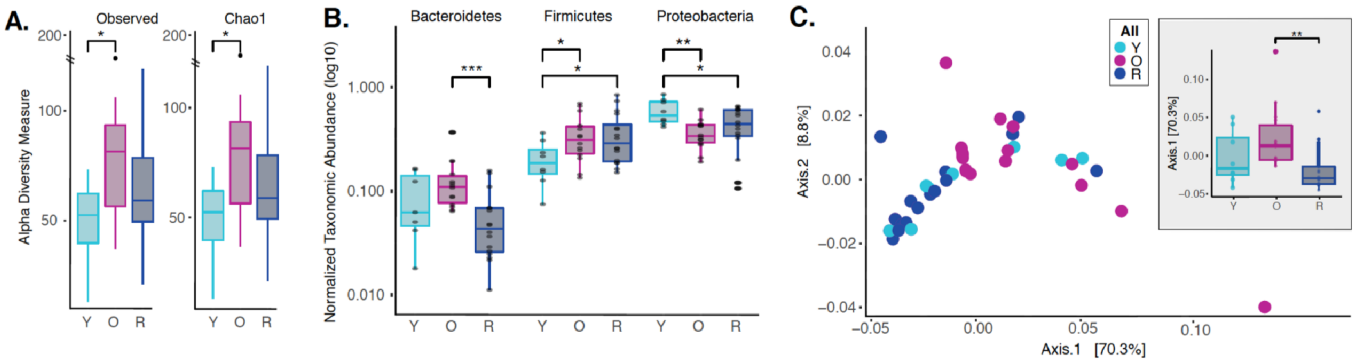

Fig. 4. Rapamycin shifts aged oral microbiome towards young oral microbiome (A) Alpha diversity for all samples reveal significant differences between young (Y) and old (O) mice without rapamycin treatment ($p<0.05$). **(B)** Phylum level abundance using normalized agglomerated data show significant difference for the *Bacteroidetes* ($p<0.001$) in old (O) mice and old mice with rapamycin treatment (R) for all samples. Also, significant changes are observed in the *Firmicutes* ($p<0.05$) and *Proteobacteria* phylum ($p<0.05$, $p<0.01$) that is age and treatment dependent. **(C)** Principal coordinate analysis using weighted unifrac distances reveal beta diversity in the rapamycin-treated old (R) groups clustered with the young (Y). **(C, inner panel)** A significant separation between old (O) and rapamycin-treated old (R) groups ($p<0.01$; Axis 1, 70.3%) was observed, but no significant difference between young (Y) and rapamycin-treated old (R) groups was observed. * $p<0.05$, ** $p<0.01$,*** $p<0.001$

SUPPLEMENTAL METHODS AND FIGURES

Rapamycin rejuvenates oral health in aging mice

Jonathan Y. An[1,2], Kristopher A. Kerns[1,6], Andrew Ouellette[3], Laura Robinson[3], Doug Morris[3], Catherine Kaczorowski[3], So-Il Park[2], Title Mekvanich[2], Alex Kang[2], Jeffrey S. McLean[1,5], Timothy C. Cox[4,*], Matt Kaeberlein[1,2]

Materials and Methods:

Animal Studies

To enhance rigor and reproducibility, experiments were performed on two different cohorts housed at two sites: the University of Washington in Seattle, WA and the Jackson Laboratory in Bar Harbor, ME. To examine the impact of rapamycin on the periodontium during normative aging, we designed a cross institutional study between the University of Washington (UW) and the Jackson Laboratory (JAX) (Supplemental Figure 1). The UW cohorts of C57BL6/JNia (hereafter termed NIA-UW Colony) were received directly from the National Institute on Aging (NIA) Aged Rodent Colony and acclimated within the UW facilities. The JAX cohorts of C57BL/6J (hereafter termed JAX Colony) were born and raised within the JAX facilities. We then treated mice at both sites with encapsulated rapamycin (eRAPA) in the diet at 42ppm, which has been shown to significantly increase lifespan of UMHET3 and C57BL6/J mice (*41, 42*), or control food (eudragit). For the NIA-UW colonies, 5 young, 5 adult, and 20 old (10 eudragit and 10 rapamycin) animals were utilized. While for the JAX colonies a total of 13 young and 26 old (13 eudragit and 13 rapamycin) animals were used. For this study, young, adult, and old mice were 6, 13, and 20 months of age, respectively.

Seattle, WA

Twenty NIA-UW mice (10 on eudragit, 10 on rapamycin) received assigned diet treatments at 20 months of age, lasting for 8 weeks, along with 5 young and 5 adult mice as normative aging controls. Animals were housed individually in Allentown NexGen Caging (Allentown, Allentown, NJ) containing corncob bedding and nestlets. Mice were fed irradiated Picolab Rodent Diet 20 #5053 (Lab Diet, St. Louis, MO). Animals were maintained in a specific pathogen free facility within a *Helicobacter spp.*-free room. Mice were housed in groups and inspected daily. National guidelines for the Care and Use of Animals and the IACUC guidelines were followed.

Bar Harbor, ME

All methods are in accordance with The Jackson Laboratory Institutional Animal Care and Use Committee (IACUC)-approved protocols. Animals were fed standard Lab Diet 6% 5K52 with eRapa at 42mg/kg/day or control. Animals were fed afternoons 1x per week, and checked daily for any animal health concerns, additional chow if needed and water was available *ad libitum*. Animals were housed at 3-5 animals per cage.

A cohort of mice were transferred into the JAX Center for Biometric Analysis and brought into the imaging suite in groups of 10 mice per scan group. Prior to scanning, the weight of each mouse was recorded and anesthesia induced with 2-3% isoflurane. The mice were then placed in a prone position in the CT scanner and kept anesthetized for the duration of the scan with an isoflurane level of 1.2-1.5%. A whole head scan was performed with bone mineral density phantoms included on the specimen positioning bed. After the CT scan, the mouse was placed in a warmed isolation cage and allowed to fully recover from the anesthesia. At the end of the imaging session, the cohort was returned to animal housing facility.

Animal experimentation was performed in accordance with the recommendations in the Guide for the Care and Use of Laboratory Animals of the National Institutes of Health. All animals were handled according to approved institutional animal care and use committee (IACUC) protocols (#4359-01) of the University of Washington and (#06005-A24) of the Jackson Laboratory.

Encapsulated Rapamycin Feeding
Encapsulated rapamycin was obtained from Rapamycin Holdings, Inc. food pellets were ground and mixed with encapsulated rapamycin at 42ppm. 300ml of 1% agar melted in sterile water, and 200ml of sterile distilled water were added per kilogram of powdered chow in order to make pellets. Pellets were stored at -20 °C until use. Control food contained the same concentration of agar and encapsulated material (eudragit) without rapamycin at the concentration that matched the rapamycin chow.

Micro-computed Tomography (μCT) Analysis

Seattle Children's Research Institute and Friday Harbor Lab Imaging Parameter and Processing
NIA-UW samples were scanned in a Skyscan 1076 and 1173 microCT system at the Small Animal Tomographic Analysis Facility (SANTA) at Seattle Children's Research Institute and Friday Harbor Laboratories at the University of Washington. Resolutions were 8-18 μm with following settings: 5 kV, 179μA, 360-ms exposure, 0.5 Al filter, 0.7° rotation step, and 3-frame averaging. Raw scan data were reconstructed with NRecon 1.6.9, and three-dimensional (3D) renderings were generated with Drishti 2.7 (Limaye 2012). For periodontal bone loss, 3D rendered images were randomized and landmarked by independent observers. Periodontal bone loss was measured as distance from the cementoenamel junction (CEJ) to alveolar bone crest (ABC) on 16 predetermined landmarks on the buccal aspect of maxillary and mandibular periodontium. The CEJ-ABC distances were totaled for each mouse through the Drishti software, and means calculated. The analysis was completed by 3-4 independent observers.

Jackson Laboratory (JAX) Imaging Parameter and Processing
The mouse is scanned in a Perkin-Elmer Quantum GX in vivo Micro-CT tomograph. Resolutions were 17-50 microns with the following settings: 55 kV, 145 μA, 4-min exposure over 360 degrees rotation. The native Perkin-Elmer Viewer VOX image files are converted to Drishti Volume Exploration and Presentation Tool NetCDF format volumes using custom code specific for this study (*43*).

Western Blot and Proteome Profile Analysis
For protein analysis by Western Blot, gingival tissue and alveolar bone was dissected. Total cellular proteins were extracted in RIPA Lysis and Extraction Buffer (Thermo Scientific, MA, USA) and EDTA-free Halt™ protease and phosphatase inhibitor cocktail included to prevent protein degradation during extraction process. Gingival tissue was pooled from co-housed animals. Protein concentration was determined by Bradford colorimetric assay (Thermo Scientific). 10-20 μg of total protein was separated by SDS-PAGE on 10% or 12% (w/v) polyacrylamide gel, then transferred to PVDF membrane using Trans-Blot Turbo Transfer System (Bio-Rad, CA, USA). Antibodies to NF-κB p65 (D14E12) XP® (8242, Cell Signaling Technology), phospho-IκB (B-9, Santa Cruz), IκB (32518, Abcam), GAPDH (D16H11) XP® (5174, Cell Signaling Technology), RANKL (G-1, sc377079, Santa Cruz), and Mouse OPG (R&D Systems, AF459) were used to probe the membrane. Dependent upon the strength of the antibody-dependent signal, either the membranes were stripped with Restore™ Plus Western Blot Stripping Buffer and reprobed for total antibody, or duplicate gels were run and separate blots probed

Analysis of the cytokine proteome was completed using a Mouse XL Cytokine Array Kit (R&D Systems, Bio-Techne Corporation, MN, USA). Gingiva and alveolar bone samples were individually pooled, protein concentration determined by a Bradford colorimetric assay, and 200μg of protein lysate loaded. Detection and imaging were performed using ChemiDoc™ XRS+ (Biorad, USA) and Image Lab Software (Biorad, USA). Data analysis was completed per the manufacture's protocol.

Histology
Tissues were fixed in Bouin's solution, and demineralized in AFS (acetic acid, formaldehyde, sodium chloride). Mandibles were processed and embedded in paraffin. Serial sections of 5 μm thickness were collected in the

coronal (buccal-lingual) plane. Sections were stained for tartrate-resistant acid phosphatase (TRAP) to examine osteoclast activity and numbers (Sigma-Aldrich Kit, St. Louis, MO, USA), and Fast Green counterstaining and examined with a Nikon Eclipse 90i Advanced Research Scope. Representative images (40x) were taken of the alveolar bone furcation.

Microbiome Analysis

DNA extraction

Mandible samples were cryogrinded and homogenized using Evolution with bead-beating tubes and ceramic beads (Bertin Instruments, Rockville, MD). Bacterial genomic DNA was extracted using the QIAamp DNA Microbiome Kit (Qiagen, Hilden, Germany) and further purified and concentrated using DNA Clean and Concentrator Kit (Zymo Research, Irvine, CA, USA) according to the manufacturer's protocol, then stored at -80˚C until all samples were collected

Sequencing

The V3-V4 variable region of the 16s ribosomal RNA gene was amplified using gene-specific primers with Illumina adapter overhang sequences (5'-TCGTCGGCAGCGTCAGATGTGTATAAGAGACAGCCTACGGGNGGCWGCAG-3' and 5'-GTCTCGTGGGCTCGGAGATGTGTATAAGAGACAGGACTACHVGGGTATCTAATCC-3'). Each reaction mixture contained 2.5 µl of genomic DNA, 5 µl of each 1 µM primer, and 12.5 µl of KAPA HiFi HotStart ReadyMix. Amplicon PCR was carried out as follows: denaturation at 95°C for 3 minutes, 35-40 cycles at 95°C for 30 sec, 55°C for 30 sec, 72°C for 30 sec, followed by a final extension step at 72°C for 5 min. PCR products were verified using gel electrophoresis (1% agarose gel) and cleaned with AMPure XP beads (Agencourt, Beckman Coulter Inc., Pasadena, CA, USA). Amplicons were then indexed using the Nextera XT Index Kit V2 set A and set D (Illumina) and purified again with AMPure XP beads to remove low molecular weight primers and primer-dimer sequences. DNA concentrations were concentration of 1-2nM using the SequalPrep™ Normalization Kit (Invitrogen). Samples were pooled into a single library which was analyzed using the TapeStation 4200 High Sensitivity D1000 assay (Agilent Technologies, Waldbronn, Germany) and Qubit High Sensitivity dsDNA assay (Thermo Fischer Scientific) to assess DNA quality and quantity. The final pooled library was then loaded on to an Illumina MiSeq sequencer with 10% PhiX spike, which served as an internal control to balance for possible low diversity and base bias present in the 16S amplicon samples, and was run for 478 cycles and generated a total of 5.68 million paired-end reads (2x239 bp).

Bioinformatics

Raw paired-end sequences were imported in to Qiime2 (v. 2019.1) and were trimmed by 15 nt from the 5' end and truncated to 239 nt for the 3' end for both the forward and reverse reads respectively. The trimmed reads were then demultiplexed and denoised using the DADA2 package (*44*). Forward reads were only used in our analysis. Taxonomy was then assigned using the feature-classifier suite trained on the and the Human Oral Microbiome Database (HOMD v. 15.1) (*45*). Samples were then filtered for taxonomic contaminants excluded samples with less than 10,000 reads. Alpha and Beta diversity as well as other analysis were done in R-Studio using the Phyloseq (*46*) Clustvis (*47*), ggplot2 (*48*), ampvis2 (*49*), vegan (*50*), ade4 (*51*) packages as part of the R suite.

Supplemental methods

Taxonomy filtered from samples was determined by analysis of kit controls with no template and zymo sequencing controls of know diversity and abundance (the QIAamp DNA Microbiome Kit (Qiagen, Hilden, Germany) DNA Clean and Concentrator Kit (Zymo Research). The following taxonomic assignments were removed as part of the dada2 workflow (*44*): Unassigned, Cyanobacteria, acidovorans, pestis, coli, flavescens, sakazakii, durans, diminuta, anthropi, monocytogenes, parasanquinis_clade_411, otitidis, subtilis, aeruginosa , fermentum.

Statistical Analysis

Results for µCT analysis, including measurements, quantitative histology, proteome analysis are expressed as mean ± standard error of mean (SEM). Data were analyzed where appropriate using Student's *t*-test or paired t-test (comparing two groups only), or one-way analysis of variance (ANOVA) with post-hoc Tukey test for multiple comparisons, where p-values < 0.05 were considered statistically significant. Statistical analysis was completed GraphPad Prism 8.00 (Graphpad, Software, La Jolla, CA, USA). For the 16s rRNA sequencing, to

identify statistically significant differences among agglomerated and normalized amplicon sequence variants (ASV) between samples as well as differences in alpha and beta diversity measures, we applied both the unpaired Wilcoxon rank-sum test as well as the two-tailed paired t-test – both with a 95% confidence interval ($\alpha = 0.05$). Alpha diversity was assessed measuring Shannon, Chao1, Observed (ASV), and Fisher diversity measures. Beta diversity was measured using weighted Unifrac distances. Statistical analysis for the microbiome analysis was completed in R (v. 3.5.3).

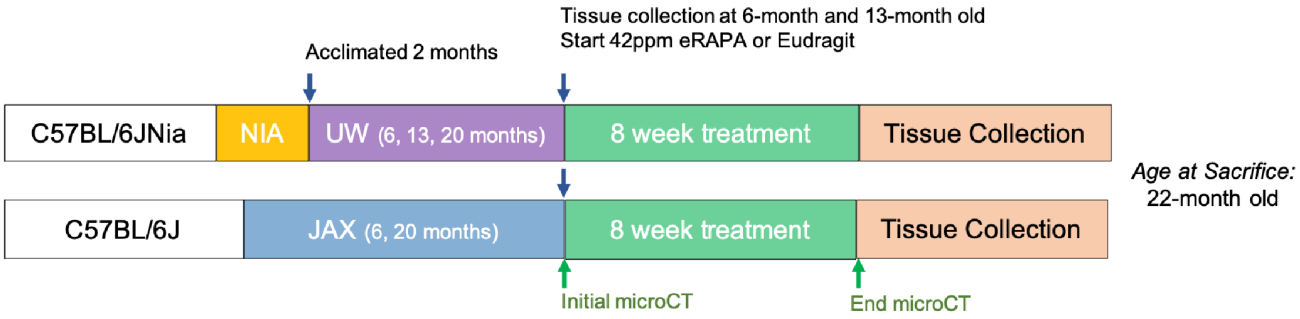

Fig. S1. **Cross-Institution Experimental Design**
The NIA-UW colonies were received directly from the NIA Aged Rodent Colony at 4, 11, and 18-months, then acclimated for two months within the UW facilities (ARCF) until they reached 6 (Young), 13 (Adult), and 20-months (Old). The Young and Adult cohorts were harvested for oral tissues and microbiome. The Old cohorts were randomized and either given Eudragit or 42ppm eRAPA within the food for 8 weeks. For the JAX colonies, an initial microCT image was taken prior to the 8-week treatment and then a final microCT before harvest. All animals were harvested at the end of 8 weeks, ~22-months old.

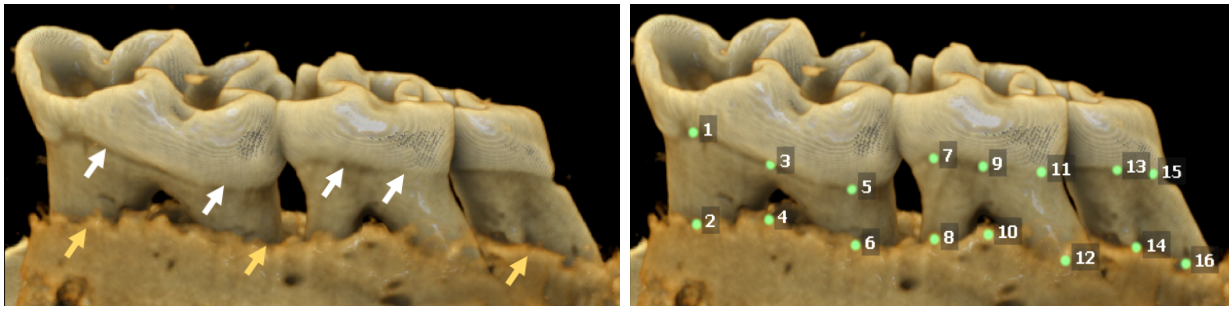

Fig. S2. Assay for Measuring Periodontal Bone Loss. Representative image of a mandible is shown. Periodontal bone loss was measured as distance from the cementoenamel junction (CEJ, white arrows) to alveolar bone crest (ABC, orange arrows) on 16 predetermined landmarks on the buccal aspect of maxillary and mandibular periodontium. The CEJ-ABC distances were totaled for each mouse.

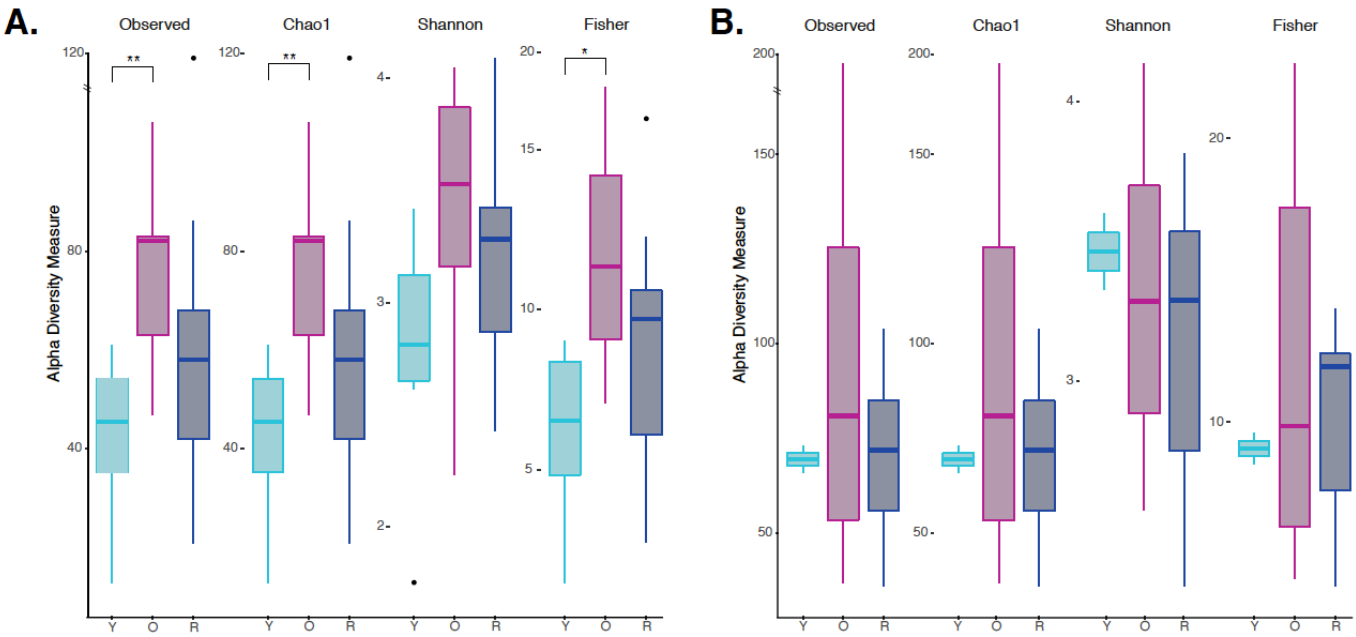

Fig. S3. Independent Alpha Diversity Analysis for JAX and UW-NIA animals. (A) Alpha Diversity measures for JAX Lab animals, including 6-month old (Y), 22-month old (O), and 22-month-old mice treated with rapamycin (R). (B) Alpha Diversity Measures for UW-NIA animals, including Y, O, and R mice. Significant differences between the different alpha diversity measures between Y and O mice, including Observed, Chao1, and Fisher, was observed among the JAX samples. No significant difference between taxonomic richness among Y and R mice was observed in JAX samples. This result was also observed independently in the UW-NIA animals. *p<0.05, **p<0.01.

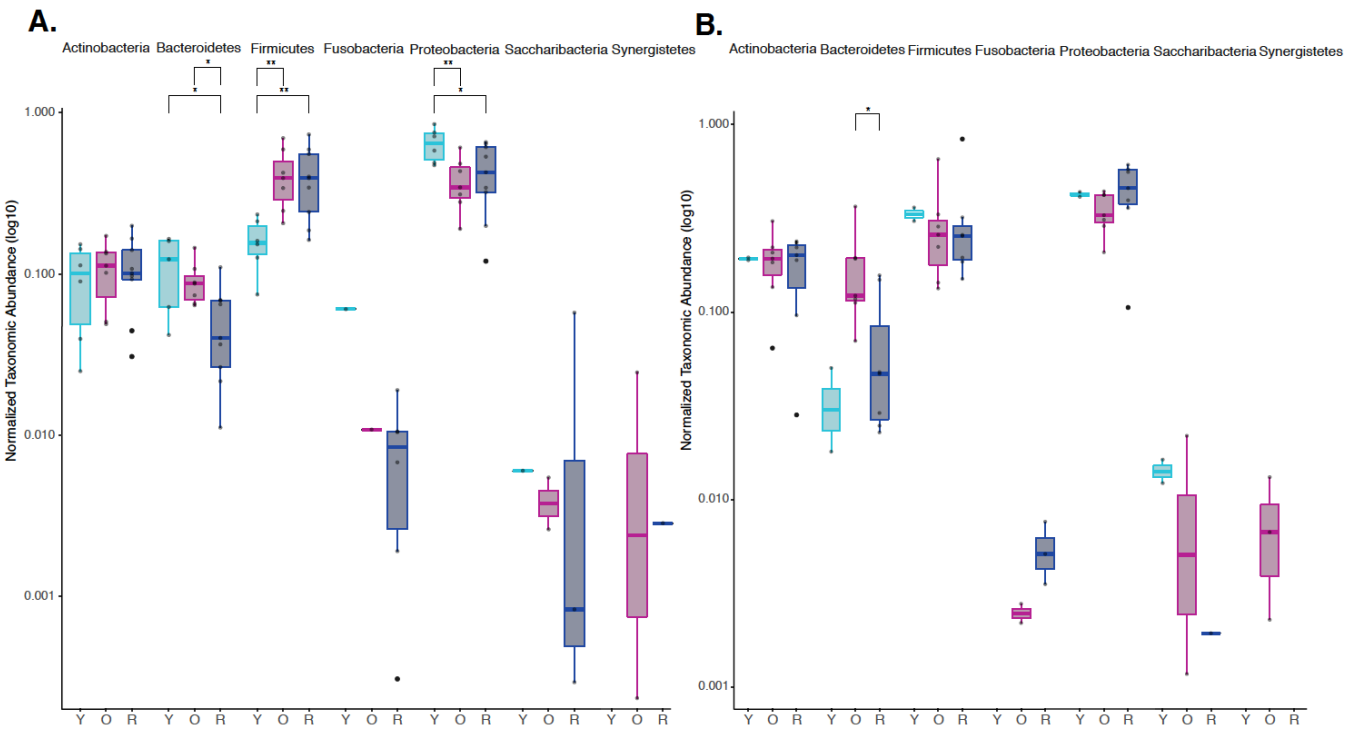

Fig. S4. Independent Phylum Level Abundance Analysis for JAX and UW-NIA animals. Normalized agglomerated data was used to evaluate phylum level abundances using an amplicon sequence variant (ASV) approach for both JAX and UW-NIA animals independently. (A) Significant differences in Bacteroidetes, Firmicutes, and Proteobacteria was observed in JAX animals, including 6-month old (Y), 22-month old (O), and 22-month-old mice treated with rapamycin (R (B) Significant differences in Bacteroidetes was observed in UW-NIA animals. * $p<0.05$, **$p<0.01$.

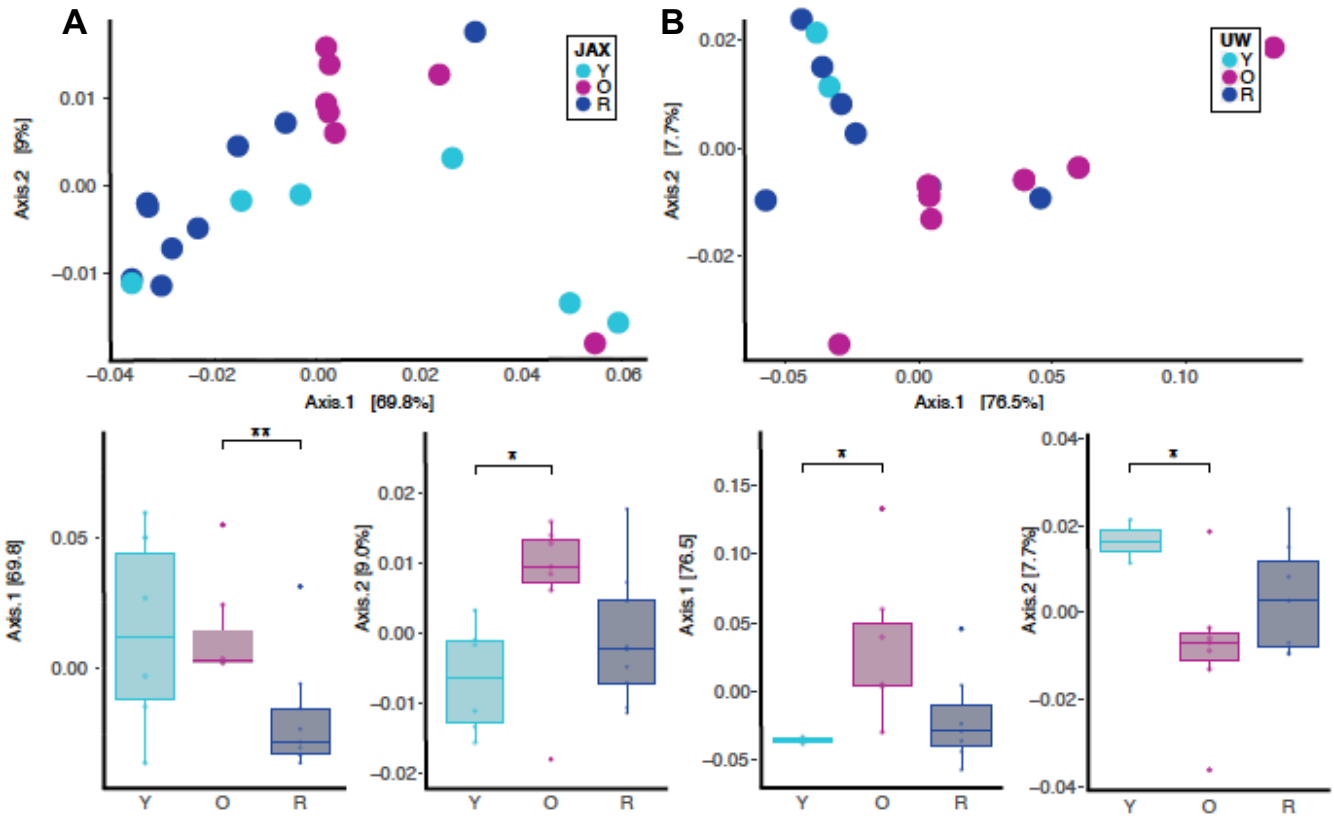

Fig. S5. Independent Beta Diversity for JAX and UW-NIA animals by Principal Coordinate Analysis using Weighted Unifrac Distances. (A) Beta diversity for only JAX samples there was significant separation between O and R ($p<0.01$; Axis 1, 69.8%) as well as between Y and O groups ($p<0.05$; Axis 2, 9.0%). **(B)** Beta diversity for only the UW samples also reveal significant difference between Y and O groups ($p<0.05$; Axis 1, 76.5%; $p<0.05$; Axis 2, 7.7%). * $p<0.05$, ** $p<0.01$